Contents lists available at Science-Gate

International Journal of Advanced and Applied Sciences

Journal homepage: https://www.science-gate.com/IJAAS.html

A regression analysis of specific printing energy and CO_2 emissions in additive manufacturing processes

Majed Masmali *

Industrial Engineering Department, College of Engineering, Northern Border University, Arar, Saudi Arabia

ARTICLE INFO

Article history:
Received 25 August 2025
Received in revised form
11 January 2026
Accepted 11 March 2026

Keywords:
Additive manufacturing
CO_2 emissions
Fused filament fabrication
Specific printing energy
Sustainability

ABSTRACT

Manufacturing processes are increasingly required to improve sustainability in order to reduce energy use and environmental impact. This study develops regression models to quantify and predict Specific Printing Energy (SPE) and CO_2 emissions in Fused Filament Fabrication (FFF) using Polylactic Acid (PLA) filament. The main objective is to optimize key printing parameters to support more efficient and sustainable additive manufacturing. A full factorial experimental design was applied, including 729 experimental runs based on six FFF parameters at three levels. Multiple linear regression models were developed using Minitab to evaluate the effects of these parameters on SPE and CO_2 emissions. Model reliability was confirmed through comprehensive statistical analysis, including analysis of variance (ANOVA), R-squared evaluation, and residual diagnostics. The results show that the models explain 89.17% of the variation in SPE and 87.37% of the variation in CO_2 emissions. Among the parameters, layer height has the strongest negative effect on both responses, while printing speed also reduces SPE and CO_2 emissions. In contrast, nozzle temperature and bed temperature have positive effects on both measures. The proposed models provide a quantitative framework for sustainability optimization in additive manufacturing and offer practical guidance for selecting printing parameters to reduce energy consumption and environmental impact.

1. Introduction

Manufacturing systems aim to produce goods economically while simultaneously prioritizing environmental sustainability. Achieving this dual objective, often termed green manufacturing, involves minimizing harmful ecological impacts and conserving energy and natural resources. Such sustainability initiatives span various production methods, including both subtractive and additive manufacturing processes. Focusing on the latter, the increasing adoption of additive manufacturing, also known as 3D printing, carries a growing imperative to understand and mitigate its environmental footprint (Anussornnitisarn et al., 2025). One of the most significant environmental impacts is energy consumption and the associated carbon dioxide emissions throughout the production lifecycle (Sideris et al., 2025).

The core concept of additive manufacturing, pioneered by Charles Hull in the 1980s (Hull, 2015), involves constructing three-dimensional objects layer by layer from digital design. This technology facilitates the production of complex geometries and bespoke designs, thereby substantially augmenting the perceived value of products (Kudus et al., 2016). As users engage in the customization of their designs, the value of these 3D printed items correspondingly increases, reflecting their distinct preferences and requirements. This trend toward personalization is significant, as it empowers end-users and enhances their overall experience in comparison to conventional mass-produced products (Hariastuti et al., 2022). Additive manufacturing encompasses various forms, such as Selective Laser Sintering (Liu et al., 2022) and Laser Powder Bed Fusion (Yuan et al., 2025). Among these, Fused Filament Fabrication (FFF) technology, established by Crump (1992), has gained widespread adoption as a 3D printing method.

The mechanism of Fused Filament Fabrication involves melting a thermoplastic filament in a heated nozzle and precisely extruding it layer by layer onto

* Corresponding Author.
Email Address: majed.masmali@nbu.edu.sa
https://doi.org/10.21833/ijaas.2026.03.014
Corresponding author's ORCID profile:
https://orcid.org/0000-0002-9646-1412

a heated build platform (Singh et al., 2020). This process requires significant electrical energy, primarily for maintaining the high temperatures of both the nozzle and the build platform (Fredriksson, 2019). Consequently, this electrical energy consumption directly contributes to CO_2 emissions, with the number of emissions being entirely dependent on the carbon intensity of the electrical grid supplying the power (Peron et al., 2024). As each layer is deposited, it cools and solidifies, bonding to the preceding one until the complete three-dimensional object is meticulously constructed (Srivastava et al., 2019).

To effectively optimize and control the Fused Filament Fabrication (FFF) process, it is essential to first understand how key printing parameters (independent variables) influence the desired outcomes (dependent variables). Therefore, a statistical analysis approach is the most suitable methodology for this investigation. This is where the Design of Experiments becomes critical; it is a key concept that systematically plans how to collect data (Montgomery, 2017). Systematically planning data collection eliminates the need for a trial-and-error approach and allows for the precise determination of each variable's influence on the final outcomes.

Recent research has significantly advanced the understanding of energy consumption and properties in additive manufacturing. A systematic literature review revealed a critical need for more accurate predictive models regarding energy consumption in metal additive manufacturing (Liu et al., 2018). Following this, another study focused on the interaction between part geometry, layer thickness, and printer type to minimize energy consumption in FFF, contributing to the development of a general prediction model despite significant limitations regarding accuracy (Manford et al., 2023). The methodologies employed in recent studies utilized Response Surface Methodology (RSM) and Central Composite Design (CCD) to investigate how printing parameters affect product characteristics, using ANOVA to identify significant factors (Dicks et al., 2024).

Similarly, other research examined the impact of printing parameters on energy consumption in FFF, employing a Taguchi L27 orthogonal array design and finding that layer height was the most influential parameter (Yi et al., 2020). An experimental study on material extrusion 3D printing with polylactic acid (PLA) employed a Taguchi L27 orthogonal array and quadratic regression models to analyze process factors.

This study provided valuable data for balancing energy efficiency and product quality, though it noted limitations in the prediction accuracy of Specific Printing Power (SPP) (Vidakis et al., 2023). In another study, researchers analyzed 13 process parameters in FDM with PLA using the Taguchi methodology, concluding that layer height and print speed are crucial for printing time, while percent filling and the number of walls significantly influence material consumption.

In a related study, researchers used statistical analysis to investigate how infill percentage and layer thickness affect the mechanical properties of PLA-graphene composite 3D prints. The results showed that these parameters significantly influence tensile and flexural strength. A key limitation of this work is that the findings are specific to the tested materials and conditions, meaning they may not be generalizable to other scenarios (Camargo et al., 2019).

A G-code-based model was developed to predict carbon emissions from 3D printing, demonstrating that optimized parameters can significantly reduce emissions, particularly in small-batch production compared to traditional injection molding (Yu et al., 2024). Following this, energy consumption in desktop FFF and Vat Polymerization was quantified using multiple linear regression to create semi-empirical models that identify effective energy-saving strategies (Hopkins et al., 2021). The integration of Design of Experiments (DOE) and 3D printing technologies was evaluated using a Project-Based Learning approach (Unzueta and Eguren, 2023). Similarly, studies have investigated and optimized Fused Deposition Modeling (FDM), identifying print speed and the number of contours as key factors affecting product quality (Durão et al., 2019).

To enhance structural models, topology and lattice optimization methods have been employed, demonstrating how these techniques can improve performance and efficiency. Studies have also combined computational material science and experimental methods to investigate thermal conditions affecting phase transformations in various materials, aiding the development of consistent processing pathways for additive manufacturing microstructures. Combined statistical approaches have been used to optimize the properties of patterns made from various materials, successfully developing predictive models (Veeman et al., 2025). Comparisons of flexural strength of FDM parts made from PLA and Acrylonitrile Butadiene Styrene (ABS) have shown that infill percentage is more influential for PLA, while layer thickness is more critical for ABS (Zisopol, 2022).

This research aims to optimize FFF processes by developing a regression model to quantify and predict Specific Printing Energy (SPE) and CO_2 emissions when printing with PLA filament. By identifying and optimizing key printing parameters, particularly for hexagonal geometries, this study seeks to enhance the efficiency and sustainability of additive manufacturing practices. Consequently, this research provides significant insights into optimizing FFF processes toward more sustainable practices.

This paper is structured as follows: it begins with an introduction, a literature review of related work, and an identification of the research gap, followed by the research aims, objectives, significance, and contributions. The next section presents the research study design, materials, and methods, followed by the results and discussion of the

research findings. Finally, the paper concludes with a summary of key insights and suggestions for future research in the field of sustainable additive manufacturing.

2. Research methodology

To achieve the purpose of this research, the study design procedure is illustrated in Fig. 1.

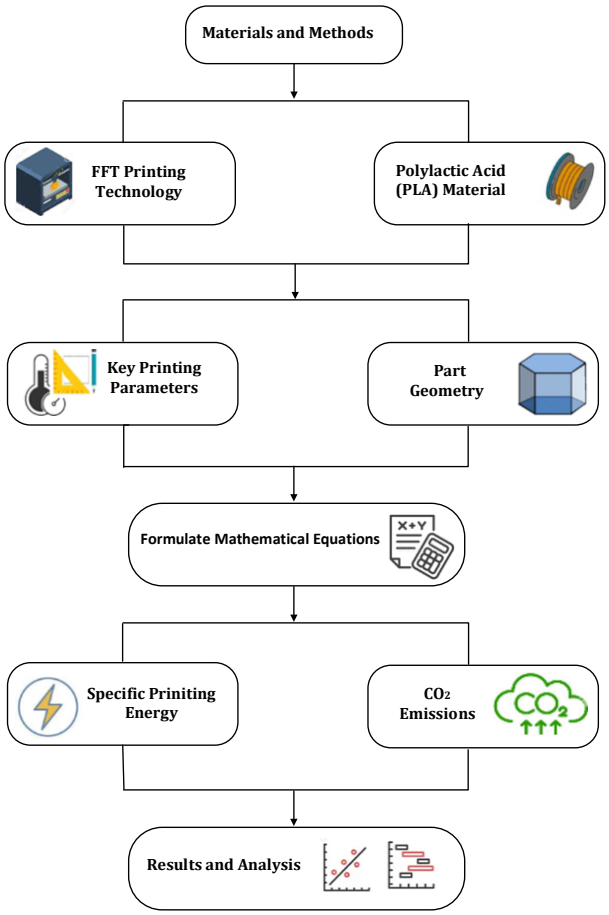

Fig. 1: Research design

Fused Filament Fabrication (FFF) was selected as the additive manufacturing technology. The material, Polylactic Acid (PLA), has its characteristics detailed in Table 1.

Table 1: Material characteristics of PLA filament (Camargo et al., 2019)

Characteristic	Value	Unit
Density	1.24×10^{-3}	g/mm³
Heat of fusion	200×10^{3}	J/kg
Melting temperature	180	˚C
Specific heat	1800	J/kg ˚C
Thermal conductivity	0.13	W/mK

A hexagonal geometry was adopted for the part design, which was critical for precise volumetric and mass calculations (Fig. 2). As shown in Fig. 2, a hexagonal cellular structure, defined by side length (a), layer height (L_h), total height (h), and wall thickness (t_w), served as the study's geometry. The part's total volume (V), infill volume (V_i), wall volume (V_w), total extruded material volume (V_e), and total mass (m) were calculated using the following standard geometric formulas:

$$V = \frac{3\sqrt{3}}{2} a^2 h. \quad (1)$$

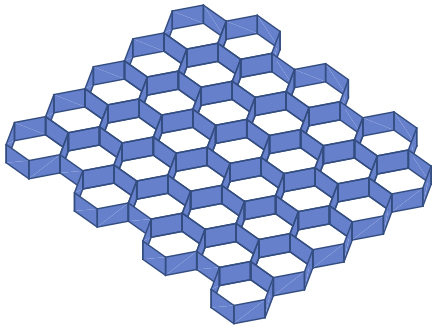

Fig. 2: Hexagonal structure

The total extruded material volume is calculated as:

$$V_e = V_i + V_w. \quad (2)$$

The total mass (m) is given by:

$$m = V_e \cdot \rho. \quad (3)$$

The printing duration (t_p) is linked to the extrusion rate by:

$$t_p = \int_0^t \frac{\kappa \cdot g(t')}{V_e} dt'. \quad (4)$$

To represent the power draw over the entire printing process, the following time-dependent power function $P_{(t)}$ is constructed:

$$P(t) = \begin{cases} P_i + P_n + P_b & \text{if } 0 \le t \le t_h \\ P_i + P_m & \text{if } t_h < t \le t_h + t_p \\ P_i & \text{if } t > t_h + t_p \end{cases} \quad (5)$$

where, P_i is idle power, P_n is nozzle power, and P_b is bed power.

To model temperature changes during printing, the energy equation is used:

$$\rho c_p \frac{\partial T}{\partial t} = \nabla \cdot (\kappa \nabla T) + q' \quad (6)$$

This equation accounts for thermal dynamics within the printed material, influencing stress and print quality.

The momentum equation is given by:

$$\rho \left(\frac{\partial u}{\partial t} + (u \cdot \nabla) u \right) = -\nabla p + u\nabla^2 \mu + \rho g. \quad (7)$$

This equation is fundamental for modeling the fluid dynamics of the molten filament during the Fused Filament Fabrication (FFF) process. It captures the balance of forces acting on the fluid, including inertial forces, pressure forces, viscous forces, and gravitational forces.

Accurately modeling these dynamics is essential for predicting how the filament will flow and behave during extrusion, which directly impacts the quality of the printed part.

To analyze the behavior of the molten filament during its cooling and solidification in the Fused Filament Fabrication (FFF) process, the constitutive equation for stress is given by:

$$\frac{d\sigma}{dt} = E\left(\frac{d\varepsilon}{dt} - \alpha\frac{d(\Delta T)}{dt}\right). \quad (8)$$

This equation describes the relationship between the rates of change of stress and strain while accounting for thermal expansion effects. Therefore, understanding these relationships is essential for enhancing print quality and ensuring the structural integrity of the printed part.

To analyze power consumption dynamics, the instantaneous power ($P_{(f)}$) is related to the time-dependent power function by:

$$P_{(f)} = \tau\frac{dP_{(t)}}{dt} + P_{(t)}. \quad (9)$$

The total energy consumed during the printing process (E_j) is evaluated through numerical integration of the power profile:

$$E_{(j)} = \sum_{i=0}^{N-1}\frac{1}{2}\left(P_{(t)} + P_{(t)}\right)\Delta t \quad (10)$$

The SPE is a key metric for evaluating the energy efficiency of the process. It is defined as the total energy consumed during printing divided by the total mass of the printed part.

$$SPE = \frac{E_{(j)}}{m} \times 10^6 \quad (11)$$

CO_2 emissions are calculated directly from the total energy consumed using an emission factor:

$$Co_2 = \left(E_{(j)} \cdot 3.6 \times 10^6\right) \cdot \left(f_{co2} \cdot 1000\right) \quad (12)$$

where, f_{CO2} is the CO_2 emission factor. For this study, the CO_2 emission factor (f_{CO2}) for the Saudi Arabian grid is set at 0.5059 kg CO_2 per kWh (Batawil and Ramdas, 2025).

The data for this regression analysis were generated through a numerical simulation approach using MATLAB software. The simulation systematically varied the six key process parameters. The printing parameters are given in Table 2.

Table 2: Printing parameters

Parameters	Values		
Bed temperature (°C)	50	60	70
Infill density (%)	10	20	30
Layer height (mm)	0.1	0.2	0.3
Layer thickness (mm)	1	1.5	2
Nozzle temperature (°C)	200	210	220
Printing speed (mm/sec)	40	60	80

For each combination of parameters, the physical and thermal models described by equations (1) through (12) were solved to obtain the corresponding energy consumption and CO_2 emission values. The experimental design was based on a full factorial configuration, with 729 unique runs derived from six factors and three levels.

Therefore, the MATLAB simulation workflow employed the following procedure: The hexagonal cellular geometry was first modeled, and a custom algorithm generated the toolpath for each run, translating kinematic parameters into time-series operational data ($P_{(t)}$). The thermal domain was meshed using the finite volume method, where the Energy Equation was solved via an implicit time-stepping scheme. The boundary conditions included fixed Dirichlet temperatures for the Nozzle and Bed that given in Table 2, and convection for heat loss on free surfaces. The total printing duration (t_p) was calculated from the toolpath and printing speed, establishing the time boundary for integrating the power profile $P_{(t)}$ to determine the total energy consumed.

3. Findings and discussion

The results from the MATLAB model have been validated against existing research, confirming the model's accuracy, reliability, and verification. This validation is crucial for ensuring precise statistical data analysis.

Fig. 3 illustrates a complete printing profile, providing a visual representation of the parameters involved. It can be noted that the total energy consumed is primarily driven by the Static Power Load required to sustain thermal components. Since the total energy is directly proportional to the total print duration, manipulating non-thermal process parameters such as Layer Height and Printing Speed offers the most impactful leverage for minimizing the overall energy footprint of the fabrication process.

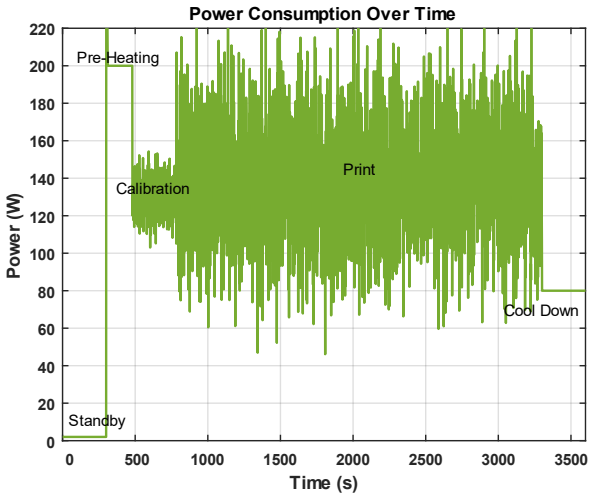

Fig. 3: Printing profile

Fig. 4 presents the relationship between specific printing energy (MJ/g) and nozzle temperature, alongside bed temperature, while keeping other parameters constant. It is evident that specific

printing energy increases with higher nozzle temperatures. This increase can be attributed to the greater thermal energy required to melt the filament more effectively at elevated temperatures, leading to higher energy consumption during the extrusion process.

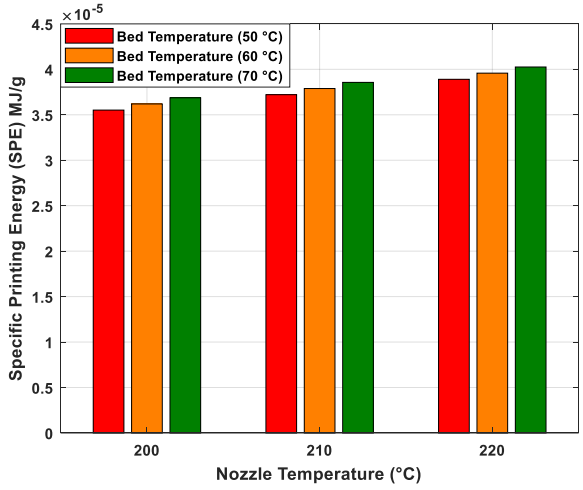

Fig. 4: Specific printing energy

As shown in Fig. 5, there is a clear inverse relationship between printing speed (mm/sec) and CO_2 emissions (g). Specifically, as printing speed increases, CO_2 emissions decrease.

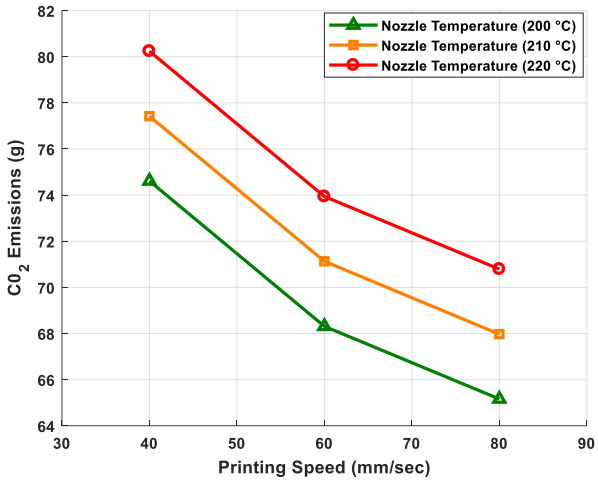

Fig. 5: CO_2 emissions

This phenomenon can be attributed to reduced dwell time of the material in the heating zone, which lowers the overall energy required for melting and extrusion. However, it is important to note that while higher printing speeds lead to lower CO_2 emissions, print quality may be affected. Conversely, increasing nozzle temperature correlates with higher CO_2 emissions due to increased energy consumption for material melting. These findings validate the simulation outputs and provide a foundation for further statistical analysis of the model.

Subsequently, statistical data analysis was performed using Minitab software, detailed in the following subsections. The multiple linear regression model for Specific Printing Energy was developed using Nozzle Temperature, Printing Speed, Bed Temperature, Layer Height, Layer Thickness, and Infill Density as predictor variables. The analysis demonstrates a highly significant and robust model. The Analysis of Variance (ANOVA) as given in Table 3 indicates that the overall regression model is highly statistically significant, with an F-value of 990.66 and an associated P-value of 0.000. This confirms that the selected process parameters collectively explain a significant portion of the variability in Specific Printing Energy.

Table 3: ANOVA for specific printing energy

Source	df	Adj SS	Adj MS	F	P
Regression	6	0.00000	0.00000	990.66	0.000
Error	722	0.00000	0.00000		
Total	728	0.00000			

df: Degrees of freedom; Adj SS: Adjusted sum of Squares; Adj MS: Adjusted mean square; F: F-statistic; P: P-value

The Model Summary presented in Table 4 further illustrates the model's strong explanatory and predictive capabilities. The R-squared (R^2) value of 89.17% signifies that approximately 89.17% of the total variation in Specific Printing Energy can be explained by the independent variables. The adjusted R-squared (R_{adj}^2) of 89.08% and the predicted R-squared (R_{pred}^2) of 88.96% are very close to the R^2, indicating that the model is robust, has excellent predictive power for new observations, and is not overfitted. The standard error of the regression (S) is 20.5289 KJ, representing the typical deviation between observed and predicted energy consumption values.

Table 4: Model summary for specific printing energy

S	R^2	$R^2_{(adj)}$	$R^2_{(pred)}$
0.0000035	89.17%	89.08%	88.96%

The estimated coefficients for each predictor, their statistical significance, and the Variance Inflation Factors (VIF) are displayed in Table 5. All six independent variables are highly statistically significant (P-value = 0.000), confirming their individual importance in predicting Specific Printing Energy. The VIF values for all predictors are 1.00, indicating a complete absence of multicollinearity, which ensures the reliability and unbiasedness of the coefficient estimates.

The regression of Specific Printing Energy is presented in Eq. 13:

$$SPE = 5.1\times10^{-5}+(7.8\times10^{-7}\times T_n)-(9.5\times10^{-7}\times S_p)+(1.5\times10^{-7}\times T_b)-(4.9\times10^{-5}\times L_h)-(1.0\times10^{-5}\times L_t)-(8.0\times10^{-7}\times D_i) \quad (13)$$

Based on the regression equation for Specific Printing Energy (SPE), the coefficients reveal the impact of each printing parameter on the energy consumed. The positive coefficients for Nozzle Temperature (7.8×10^{-7}) and Bed Temperature (1.5×10^{-7}) indicate that increasing these temperatures leads to a slight rise in SPE, as more energy is required to heat and maintain them. Conversely, the negative coefficients for Printing Speed (-9.5×10^{-7}), Layer Height (-4.9×10^{-5}), Layer Thickness (-1.0×10^{-5}), and Infill Density (-8.0×10^{-7})

suggest that increasing these parameters reduces SPE.

This is primarily because faster speeds and larger layer dimensions can shorten the overall printing time, thereby decreasing the total energy consumption. Among these, the Layer Height coefficient has the most significant magnitude, indicating its strong influence on SPE.

Table 5: Coefficients for specific printing energy

Term	C_{oef}	SE C_{oef}	T-Value	P-Value	VIF
Constant	0.000051	0.00000639	7.98	0.000	
T_n	0.00000078	0.0000000363	21.51	0.000	1.00
S_p	-0.00000095	0.0000000282	-33.63	0.000	1.00
T_b	0.00000015	0.0000000174	8.6	0.000	1.00
L_h	-0.000049	0.000000925	-53	0.000	1.00
L_t	-0.00001	-0.000000493	20.3	0.000	1.00
D_i	-0.0000008	-0.000000077	10.39	0.000	1.00

Regression Analysis for CO_2 Emissions (g). The multiple linear regression model for CO_2 Emissions (g) was developed using the same set of process parameters as for Energy Consumption. The analysis reveals a similarly strong and significant relationship.

The residual plots for Specific Printing Energy (SPE) provide critical insights into the regression model's performance and validate its underlying assumptions (Fig. 6). The normal probability plot indicates that the residuals are approximately normally distributed, as the points closely follow the diagonal reference line. This supports the normality assumption essential for linear regression. The scatter plot of residuals against fitted values reveals no discernible pattern, suggesting homoscedasticity, where the variance of residuals remains consistent across fitted values. Additionally, the histogram of residuals exhibits a bell-shaped distribution centered around zero, further confirming normality. The plot of residuals versus observation order shows a random scatter around zero, indicating no autocorrelation among the residuals. Collectively, these findings affirm that the regression model for predicting SPE is statistically sound and effective for optimizing additive manufacturing processes.

The Analysis of Variance (ANOVA) results in Table 6 for CO_2 Emissions also indicate a highly statistically significant overall model (F-value = 832.79, P-value = 0.000), confirming that the process parameters collectively explain a significant portion of CO_2 emission variability.

Table 6: ANOVA for CO_2 emissions (g)

Source	df	Adj SS	Adj MS	F	P
Regression	6	41584.8	6930.8	832.79	0.000
Error	722	6008.8	8.3		
Total	728	47593.6			

The model summary in Table 7, for CO_2 Emissions, shows an R-squared (R^2) value of 87.37%, indicating that 87.37% of the variation in CO_2 Emissions is explained by the model. The adjusted R^2 (R_{adj}^2) of 87.27% and predicted R^2 (R_{pred}^2) of 87.12% are very close, affirming the model's robustness and strong predictive power. The standard error of the regression (S) is 2.88486 g. The Coefficients Table 8 for CO_2 Emissions shows that all six independent variables are highly statistically significant predictors (P-value = 0.000). All VIF values are 1.00, confirming the absence of multicollinearity and the reliability of the coefficient estimates.

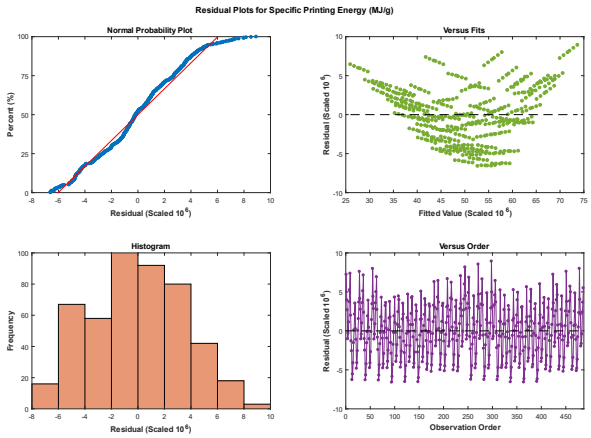

Fig. 6: Residual plots for specific printing energy consumption

Table 7: Model summary for CO_2 emissions (g)

S	R^2	R^2(adj)	R^2(pred)
2.88486	87.37%	87.27%	87.12%

The regression equation for CO_2 Emission is presented in Eq. 14:

$$CO_2 \text{ Emission} = 23.31 + 0.2814\ T_n - 0.22007\ S_p + 0.1126\ T_b - 69.35\ L_h + 2.657\ L_t + 0.1359\ D_i \quad (14)$$

The interpretation of coefficients for CO_2 Emissions largely mirrors that for Energy Consumption, indicating that process parameters influencing energy use similarly affect CO_2 output. Notably, Layer Height again has the strongest negative impact, implying that increasing it significantly reduces CO_2 emissions.

The Residual Diagnostics for CO_2 Emissions are shown in Fig. 7. Similar to the Energy Consumption model, initial analyses identified unusual observations in the CO_2 Emissions data. After thorough data verification and necessary corrections, the diagnostic plots for CO_2 Emissions residuals (Normal Probability Plot, Residuals vs. Fits, Histogram of Residuals, and Residuals vs. Order) demonstrated excellent adherence to regression assumptions, confirming normality, homoscedasticity, and independence of residuals.

Table 8: Coefficients for CO_2 emission (g)

Term	C_{oef}	SE C_{oef}	T-value	P-value	VIF
Constant	23.31	2.92	7.98	0.000	
T_n	0.2814	0.0131	21.51	0.000	1.00
S_p	-0.2200	0.00654	-33.63	0.000	1.00
T_b	0.1126	0.0131	8.60	0.000	1.00
L_h	-69.35	1.31	-53.00	0.000	1.00
L_t	2.657	0.131	20.30	0.000	1.00
D_i	0.1359	0.0131	10.39	0.000	1.00

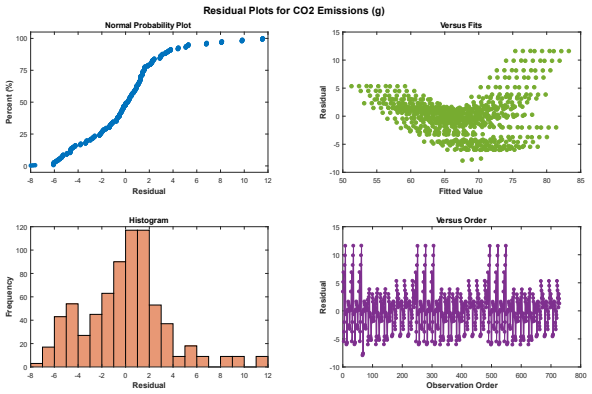

Fig. 7: Residual plots for CO_2 emission

The consistent and strong findings across both Energy Consumption and CO_2 Emissions models provide compelling insights into the environmental footprint of additive manufacturing. The identical statistical metrics and similar coefficient patterns highlight that the investigated process parameters are common drivers for both energy consumption and associated carbon emissions.

The analytical findings derived from the regression models are visually corroborated by the multi-objective response surface presented in Fig. 8.

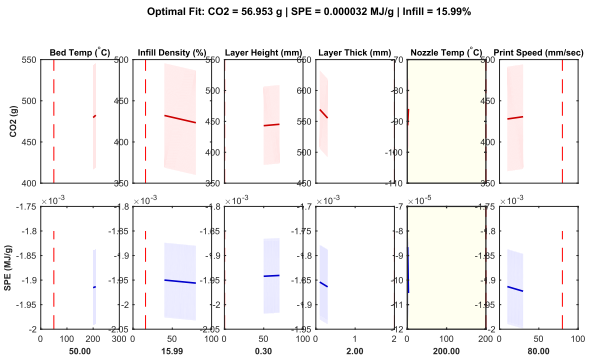

Fig. 8: Optimization plots

These optimization plots explicitly illustrate the marginal effect of varying each input parameter on the predicted SPE and CO_2 emission responses. Critically, the response profiles corresponding to Layer Height and Printing Speed exhibit the most pronounced negative slopes, empirically establishing them as the dominant control variables for minimization. This graphical evidence directly substantiates the results of the regression analysis, which quantified these factors with the largest substantial negative coefficients and provides the empirical justification for their maximal setting in the subsequent optimization routine. Key Drivers for Sustainability: Parameters such as Layer Height emerge as critical levers for sustainability optimization. The substantial negative coefficients for Layer Height in both models indicate that increasing layer height significantly reduces both energy consumption and CO_2 emissions.

Table 9 presents the optimal process parameters derived from the optimization objective (minimizing SPE and CO_2 emissions). The selected settings reflect a direct application of the regression and graphical findings.

Table 9: Optimal process parameters

Variable	Setting
Bed temperature (°C)	50
Infill density (%)	15.9912
Layer height (mm)	0.3
Layer thickness (mm)	2
Nozzle temperature (°C)	200
Printing speed (mm/sec)	80

The optimization routine strategically maximized the two factors with the most substantial negative impact on energy consumption: Layer Height (set to its maximum of 0.3 mm) and Printing Speed (set to its maximum of 80 mm/sec). Conversely, thermal parameters were set to their lower boundaries: Bed Temperature (50 °C) and Nozzle Temperature (200 °C), reflecting their positive correlation with energy use. The resulting low settings for Infill Density (≈16%) and Layer Thickness (2 mm) also contribute to the minimal energy consumption required to form the part. This suggests that for applications where feature resolution is not the primary concern, optimizing for larger layer heights can yield considerable environmental benefits.

The predictive reliability and robustness of the developed CO_2 Emissions and SPE models against the optimal set of process parameters is statistically affirmed by the final validation results presented in Table 10.

The validation for the CO_2 Emissions model confirms its strong predictive capability. The narrow 95% Confidence Interval (CI) of (56.333, 57.573) signifies the certainty around the true mean emission value, confirming the model's statistical precision. The results for the SPE model underscore the exceptional precision achieved for this metric, evidenced by the extremely small SE Fit (0.00000001). This confirmation of robustness makes the models highly suitable tools for predictive optimization and process control.

Analysis showed that Layer Height has the most substantial negative impact on both Specific Printing Energy (SPE) and CO_2 emissions. This strong correlation is explained by the fundamental physics of Fused Filament Fabrication (FFF) energy

consumption: the Static Power Load. Since most of the energy is consumed by the Heated Build Bed and the Heated Nozzle to maintain temperature continuously throughout the print duration, increasing Layer Height dramatically reduces the total number of layers, thereby minimizing the time the system spends running against this high, sustained static load.

Table 10: Multiple response prediction at optimal settings

Response	Fit	SE Fit	95% CI	95% PI
CO_2 emissions	56.953	0.316	(56.333, 57.573)	(51.255, 62.650)
SPE	0.000032	0.00000001	(0.000032, 0.000033)	(0.000025, 0.000039)

Fit: Predicted value; SE Fit: Standard error of the fitted value; 95% CI: 95% confidence interval; 95% PI: 95% prediction interval; SPE: Specific printing energy

However, the pursuit of maximum energy efficiency through high Layer Height and high Printing Speed introduces severe practical trade-offs. Increasing Layer Height compromises inter-layer mechanical strength and surface resolution due to diminished thermal fusion between layers. For functional parts, the practical upper limit for Layer Height is often around 0.2 mm, as exceeding this leads to unacceptable anisotropy and poor structural integrity. Similarly, increasing Printing Speed must be tempered, as it introduces defects in dimensional accuracy and further degrades layer fusion.

To overcome these trade-offs, parameters with a positive correlation to energy, such as Nozzle Temperature and Bed Temperature, must be utilized as necessary compensatory variables. If high speed and high layer height are chosen for sustainability, a calculated increase in Nozzle Temperature becomes necessary to restore adequate thermal energy for robust layer adhesion. Likewise, increasing the Bed Temperature consumes additional energy but is essential for controlling warping and preserving the part's dimensional accuracy. Ultimately, these quantitative models provide an effective framework for Process Optimization, shifting the focus from achieving the absolute minimum SPE to reaching the minimum Specific Printing Energy required to satisfy the part's critical quality and mechanical durability constraints, ensuring that the manufactured products are both environmentally responsible and functionally viable.

4. Conclusions

To sum up, this study presents a comprehensive statistical analysis aimed at predicting sustainability metrics, with a specific focus on two critical impacts: specific printing energy and CO_2 emissions in additive manufacturing processes. The model effectively demonstrates a significant correlation between six key printing parameters and these sustainability impacts, revealing that optimizing these parameters can lead to enhanced energy efficiency and reduced carbon footprints.

This research contributes to the field of sustainable additive manufacturing through a quantitative framework that allows practitioners to make informed decisions regarding the optimization of FFF processes. Identifying key parameters that influence energy consumption and emissions offers actionable insights for manufacturers seeking to align their practices with sustainability goals. While the research is constrained with the use of numerical simulations, FFF technology, hexagonal geometry, and PLA materials, these limitations highlight important avenues for future investigation. Future studies could explore alternative materials, geometries, and printing techniques to further improve sustainability outcomes. Additionally, integrating renewable energy sources into the manufacturing process could further enhance sustainability and align with green manufacturing practices.

Moreover, insights gained from this analysis can guide practitioners in making informed decisions that align with sustainability goals. Overall, statistical analysis not only interrelates the six key printing parameters but also contributes valuable knowledge to the field of additive manufacturing. Addressing the identified limitations and pursuing the suggested avenues for future research can advance the industry significantly toward more sustainable practices and manufacturing.

Nomenclature

a	Side length
c_p	Specific heat
D_i	Infill density (%)
E	Young's modulus
$E_{(j)}$	Total energy consumption
f_{CO2}	CO_2 emission factor
g	Gravity vector
$g(t')$	Time function
h	Hexagon height
H_f	Heat of fusion
k	Thermal conductivity
L_h	Layer height (mm)
L_t	Layer thickness (mm)
m	Mass
N	Time steps
p	Pressure
$P_{(t)}$	Power profile
P_b	Bed power
P_f	Target power
P_i	Idle power
P_m	Motion power
P_n	Nozzle power
q'	Heat generation rate
SPE	Specific printing energy
S_p	Printing speed (mm/sec)
t	Time
T_b	Bed temperature (∘C)
t_{end}	End time
t_h	Total heat time
t_i	Time step
T_m	Melting temperature
T_n	Nozzle temperature (∘C)
t_p	Print duration

t_w Wall thickness
u Fluid velocity
V Hexagon volume
V_e Extruded volume
V_i Infill volume
V_r Volumetric rate
W_v Wall volume
α Thermal expansion coefficient
Δt Time step size
ΔT Temperature change
ϵ Strain
μ Dynamic viscosity
∇ Nabla operator
ρ Material density
σ Mechanical stress
τ Time constant

Compliance with ethical standards

Conflict of interest

The author(s) declared no potential conflicts of interest with respect to the research, authorship, and/or publication of this article.

References

Anussornnitisarn P, Nivasanon C, Kim N, and Ransikarbum K (2025). Sustainable technology selection in additive manufacturing: an integrated fuzzy decision analysis framework. The International Journal of Advanced Manufacturing Technology, 138: 1177–1196. https://doi.org/10.1007/s00170-025-15572-1

Batawil MA and Ramdas SK (2025). Fuzzy logic controlled PV microgrid for a sports complex in Saudi Arabia. European Journal of Engineering and Technology Research, 10(3): 43-53. https://doi.org/10.24018/ejeng.2025.10.3.3269

Camargo JC, Machado ÁR, Almeida EC, and Silva EFMS (2019). Mechanical properties of PLA-graphene filament for FDM 3D printing. The International Journal of Advanced Manufacturing Technology, 103: 2423-2443. https://doi.org/10.1007/s00170-019-03532-5

Crump S (1992). The extrusion process of fused deposition modeling. U.S. Patent Application No. 5121329.

Dicks JA, Hoosain MI, and Mbele O (2024). Multi-objective parametric optimisation of masked stereolithography additive manufacturing using the response surface method. South African Journal of Industrial Engineering, 35(4): 52-65. https://doi.org/10.7166/35-4-3147

Durão LFC, Barkoczy R, Zancul E, Lee Ho L, and Bonnard R (2019). Optimizing additive manufacturing parameters for the fused deposition modeling technology using a design of experiments. Progress in Additive Manufacturing, 4: 291-313. https://doi.org/10.1007/s40964-019-00075-9

Fredriksson C (2019). Sustainability of metal powder additive manufacturing. Procedia Manufacturing, 33: 139-144. https://doi.org/10.1016/j.promfg.2019.04.018

Hariastuti NLP, Santoso PB, and Tama IP (2022). Identifying driving factors of technological innovation to create sustainable value in metal manufacturing SMEs. Industrial Engineering & Management Systems, 21(1): 43-57. https://doi.org/10.7232/iems.2022.21.1.043

Hopkins N, Jiang L, and Brooks H (2021). Energy consumption of common desktop additive manufacturing technologies. Cleaner Engineering and Technology, 2: 100068. https://doi.org/10.1016/j.clet.2021.100068

Hull CW (2015). The birth of 3D printing. Research-Technology Management, 58(6): 25-30.

Kudus SIA, Campbell RI, and Bibb R (2016). Customer perceived value for self-designed personalised products made using additive manufacturing. International Journal of Industrial Engineering and Management, 7(4): 183. https://doi.org/10.24867/IJIEM-2016-4-121

Liu X, Wang J, Zhu J, Liew PJ, Li C, and Huang C (2022). Ultrasonic abrasive polishing of additive manufactured parts: An experimental study on the effects of process parameters on polishing performance. Advances in Production Engineering & Management, 17(2): 193–204. https://doi.org/10.14743/apem2022.2.430

Liu ZY, Li C, Fang XY, and Guo YB (2018). Energy consumption in additive manufacturing of metal parts. Procedia Manufacturing, 26: 834-845. https://doi.org/10.1016/j.promfg.2018.07.104

Manford D, Budinoff HD, Callaghan BJ, and Jeon Y (2023). Towards a general model to predict energy consumption for fused filament fabrication. Manufacturing Letters, 35: 1358-1365. https://doi.org/10.1016/j.mfglet.2023.08.114

Montgomery DC (2017). Design and analysis of experiments. 9th Edition, John Wiley & Sons, Inc., Hoboken, USA.

Peron M, Agnusdei L, Miglietta PP, Agnusdei GP, Finco S, and Del Prete A (2024). Additive vs conventional manufacturing for producing complex systems: A decision support system and the impact of electricity prices and raw materials availability. Computers & Industrial Engineering, 194: 110406. https://doi.org/10.1016/j.cie.2024.110406

Sideris I, Yan Y, Duncan S, Afrasiabi M, and Bambach M (2025). Scalable path planning and reduced order modeling for temperature optimization in direct energy deposition. Additive Manufacturing, 109: 104831. https://doi.org/10.1016/j.addma.2025.104831

Singh S, Singh G, Prakash C, and Ramakrishna S (2020). Current status and future directions of fused filament fabrication. Journal of Manufacturing Processes, 55: 288-306. https://doi.org/10.1016/j.jmapro.2020.04.049

Srivastava M, Rathee S, Maheshwari S, and Kundra TK (2019). Additive manufacturing: Fundamentals and advancements. 1st Edition, CRC Press, Boca Raton, USA. https://doi.org/10.1201/9781351049382

Unzueta G and Eguren JA (2023). Implementation of project-based learning for design of experiments using 3D printing. Journal of Industrial Engineering and Management, 16(2): 263-274. https://doi.org/10.3926/jiem.5254

Veeman D, Bhattacharjee B, and Vellaisamy M (2025). Investigation and optimisation of mechanical properties of additively manufactured PMMA patterns using Taguchi and RSM approach. Jordan Journal of Mechanical & Industrial Engineering, 19(2): 457–468. https://doi.org/10.59038/jjmie/190216

Vidakis N, Petousis M, Karapidakis E, Mountakis N, David C, and Sagris D (2023). Energy consumption versus strength in MEX 3D printing of polylactic acid. Advances in Industrial and Manufacturing Engineering, 6: 100119. https://doi.org/10.1016/j.aime.2023.100119

Yi L, Chen T, Ehmsen S, Gläßner C, and Aurich JC (2020). A study on impact factors of the energy consumption of the fused deposition modeling process using two-level full factorial experiments. Procedia CIRP, 93: 79-84. https://doi.org/10.1016/j.procir.2020.03.036

Yu S, Liu H, Zhao G, Zhang H, Hou F, and Xu K (2024). A code-based method for carbon emission prediction of 3D printing: A case study on the fused deposition modeling (FDM) 3D printing and comparison with conventional approach. Journal of Cleaner Production, 484: 144341. https://doi.org/10.1016/j.jclepro.2024.144341

Yuan J, Guo Q, Clark SJ, Escano LI, Nabaa A, Qu M, Huang J, Li Q, Román AJ, Osswald TA, Fezzaa K, and Chen L (2025). Revealing mechanisms of processing defect mitigation in laser

powder bed fusion via shaped beams using high-speed X-ray imaging. International Journal of Machine Tools and Manufacture, 204: 104232. https://doi.org/10.1016/j.ijmachtools.2024.104232

Zisopol DG (2022). A statistical approach of the flexural strength of PLA and ABS 3D printed parts. Engineering, Technology & Applied Science Research, 12(2): 8248–8252. https://doi.org/10.48084/etasr.4739